Numerical Methods in Civil Engineering

Calculation of slip surface displacement in earth slopes using the limit equilibrium method

Zeinab. Mirzazadeh[*]*, Mohammad. Hajiazizi*[**]

ARTICLE INFO

Article history:
Received:
March 2018.
Revised:
July 2018.
Accepted:
September 2018.

Keywords:
Displacement of slope; Limit equilibrium method; Earth slope; Safety factor; Hyperboli model.

Abstract:

In the present study, shear displacements were calculated for all failure surface slices in earth slopes using the limit equilibrium method. To this end, the hyperbolic shear stress-strain constitutive law was applied. Local factors of safety were determined for the slices based on stress and displacement values. In order to calculate the displacement of earth slopes using the proposed method, a numerical model was developed satisfying the equilibrium of forces by a trial and error approach. A comparison between shear displacements obtained from this study in examples 1 and 2, with those obtained from FEM analysis which has yielded the normal errors of about 1.066% and 0.52%, respectively. Eventually, the effects of failure ratio (R_f), and hyperbolic stiffness parameters (n and k) on displacement of earth slopes were examined.

1. Introduction

Slope instability is considered as a serious challenge for civil engineers. There are various methods proposed for slope stability analysis, e.g. limit equilibrium, numerical methods, etc [1]. Due to its simplicity inexpensiveness and time-saving facilitation, the slope stability analysis by application of the limit equilibrium method is one of the most commonly implemented and highly acknowledged techniques in scientific studies [2-6]. Limit equilibrium methods assume a slip surface for which a factor of safety is calculated. However, this method does not provide any information about displacement of the slip surface. This problem can be resolved by the applied numerical methods. Recently, some novel slice methods have been proposed based on the limit equilibrium which can be used in obtaining the useful information about shear displacements along failure surfaces. In these methods, a local factor of safety can also be obtained for each slice based on stress and displacement. Therefore, it is practically important to further develop the slice methods in order to determine displacement of earth slopes. The present study was conducted engaging this point of view.

* *M.Sc Student, Razi University, Taq_e Bostan, Kermanshah, Iran.*

** *Corresponding Author: Associate Professor, Razi University, Taq_e Bostan, Kermanshah, Iran. Email: mhazizi@yahoo.com*

Hung [7] has used the generalized Janbu's method with force and moment's principles of equilibrium equations considering the Mohr-Coulomb failure criterion. He determined the displacement at the slope crest using the hyperbolic model and considering the displacement compatibility between slices. Hung [8] determined the displacement of slopes based on the principle of forces in equilibrium using the results obtained from reinforced slopes subjected to the occurred earthquake forces. A reasonable cross-match was then observed between the measured practically and calculated numerically displacements. Hung et al. [9] showed that the use of Fellenius's method yields some conservative results. They also found that the value of displacement calculated by the simplified Bishop's method was highly compatible with the observed displacement. Mohammadi and Taiebat [10] proposed a numerical method for post-failure analysis of slope displacement. Cheng and Zhou [11] proposed a novel limit equilibrium method to determine the displacement and three-dimensional stability of landslides. Ghanbari et al. [12] proposed a new formulation based on the limit equilibrium and using the horizontal slices method for estimation of the seismic displacements of a reinforced slope under earthquake loads.

Gao and He [13] proposed a new prediction method based on a new evolutionary neural network. They verified it through two real engineering applications, the analysis of three main methods and the new evolutionary neural

network method. Zhang et al. [14] studied the deformation and failure characteristics of the Liujiawan high embankment slope and sheet-pile wall. They analyzed the factors influencing instability, and established the correlation of deformation rate of the anti-slide plies and each factor having multivariate linear regression analysis. The results showed that: (1) The length of anchoring segment is not long enough, and displacement directions of embankment and retaining structure are perpendicular to the path of the highway; (2) The length of the cantilever segment is so tall that the active earth pressures behind the piles are largely. Aminpour et al. [15] studied displacements of earth slopes in the vicinity of a surcharge using the limit analysis method as well as upper bound theory within the non-associated flow rule. They suggested a new formulation for calculation of the permanent displacements of the earth slope in the presence of a surcharge for two failure modes of rotational and transitional. Hasani et al [16] simulated the dam foundation using transition spring and presented an equation for calculation of the vibrational natural frequency of earthfill dam using analytical methods. The advantages of the method are of more accurate estimation of seismic parameters as well as considering the flexibility of earth dams. Riley approximation method within shear-free shape function was used in obtaining the new correlation equation followed by step-by-step mathematical solving procedure. Macedo et al. [17] proposed a straightforward performance-based seismic slope assessment procedure, which considers a full range of potential IM (intensity measure) values to estimate the seismic slope displacements in a direct relation to a level of hazard. Seismic performance is assessed through either a Newmark-type seismic displacement estimate or a calibrated seismic coefficient that can be used in pseudo-static analyses. The relevant procedures were developed for a wide range of earth structural systems for shallow crustal earthquakes and subduction zone earthquakes. Currently employed simplified slope displacement procedures do not provide consistent assessments of the actual seismic slope displacement hazard. The proposed procedures can be readily used in practice in order to perform rigorous performance-based seismic slope displacement hazard assessments. Kokusho [18] conducted nonlinear numerical analyses wherein the Newmark-type slope model is shaken underneath by propagating SH wave. Wave energy as the difference between upward and downward SH wave is confirmed to contribute to slope sliding together with other associated energies. Residual slope displacements δr are uniquely evaluated from the wave energy despite the difference in earthquake waves, indicating that δ_r can be readily obtained with no need of acceleration time-histories. An evaluation procedure has been developed by using a set of the nonlinear analysis and empirical formulas on earthquake wave energies. Liu et al [19] proposed a slope displacement prediction model and an early warming framework based on a set of sequential intelligent computing algorithms that could take advantages of Rough Set theory (RS), Kernel principal component analysis (KPCA), quantum particle swarm optimization (QPSO), least square support vector machine (LSSVM), and Markov chain (MC). After this process, RS is utilized to identify the important influence factors in order to eliminate the multi-collinearity and redundancy of the attributes that were selected initially. As the extracted parameters are still in a high-dimensional order, KPCA is employed to fuse them into a comprehensive indicator to further reduce input dimensions and computational costs. The nonlinear relativeness model between the indicator and displacement is established by using LSSVM, with the parameters are optimized through QPSO that has much faster and better global searching ability. Once the QPSO-LSSVM model is established, MC is integrated to refine the prediction results. In the present study, the limit equilibrium method is used to calculate shear displacements along failure surface of earth slope. The local factor of safety based on stress and displacement was calculated for failure surface instead of a constant factor of safety. In addition, the hyperbolic stress-strain constitutive law was used and eventually, shear displacements were obtained for all slices as well as the slope crest. This algorithm was developed by FORTRAN programming language.

2. Calculation of slope displacement

2.1 Methodology

Initially, the safety factor was calculated for the slope by the simplified Janbu's method. Afterwards, the safety factor for each slice was calculated from the hyperbolic equation based on vertical displacement at the slop crest. Vertical displacement at the slope crest, (Δ_0), was obtained from the force equilibrium equation, $(\sum F_H = 0)$. This procedure was continued in the form of a repetitive algorithm until a reasonable convergence was achieved. Moreover, the resulted displacement was considered as the vertical displacement of the slope crest. The Atkinson displacement compatibility equation (Atkinson, 1981) was used to calculate the shear displacement at the bottom of each slice. Thereinafter, the factor of safety was calculated based on the stress and displacement for each slice. Fig. 1 illustrates the failure surface and the forces acting on a slice.

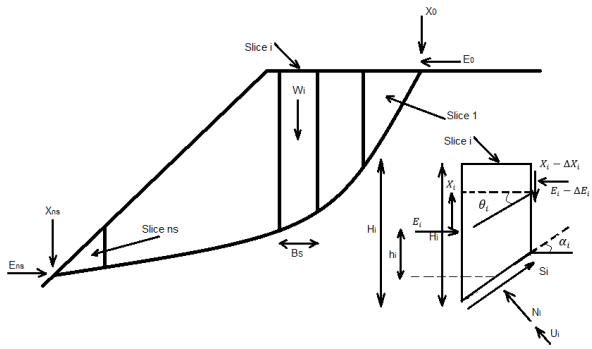

Fig. 1: Forces acting on a slice with a non-circular failure surface

2.2 Calculation of factor of safety using the simplified Janbu's method

The simplified Janbu's method [20] used to calculate the factor of safety is as follows:

$$F_S = \frac{\sum (S_{fi}.\sec\alpha_i)}{\sum [W_i] - E_{ns} + E_0} \tag{1}$$

$$S_{fi} = (S_{fi})_{\text{residual}} = \frac{C_i + (W_i - U_i\cos\alpha_i).\tan\phi.\sec\alpha_i}{1 + \frac{\tan\phi.\tan\alpha_i}{F_S}} \tag{2}$$

$$(S_{fi})_{mobilizied} = \frac{S_{fi}}{F_S} = \frac{(S_{fi})_{residual}}{F_S} \tag{3}$$

$$C_i = c_i.l_i = c_i.B_i.\sec\alpha_i \tag{4}$$

$$U_i = u_i.l_i = u_i.B_i.\sec\alpha_i \tag{5}$$

Where
i = slice number (i = 1,2, … , ns)
l_i , B_i = length and width of slice i, respectively.
W_i = weight of slice
α_i = inclination angle of the base of slice i
$\emptyset$ = internal friction angle
E_0 , E_{ns} = Horizontal forces at the first and end of the failure wedge, respectively.

$$F_{S_{Ordinary}} = \frac{\sum [C_i + W\cos\alpha_i\tan\phi]}{\sum W\sin\alpha_i} \tag{6}$$

The convergence of FS is checked using the Eq. (7) as follows:

$$F_S = \frac{(F_S)_{new} - (F_S)_{old}}{(F_S)_{new}} \le 0.01 \tag{7}$$

2.3 Janbu's method in terms of displacement

The factors of safety based on local forces (FS_i) and the hyperbolic stress-strain model are substituted in the simple Janbu's equation resulting in a definite static system. Considering the normal force acting on the slice i ($\acute{N}_i$), equilibrium of forces in the vertical direction is expressed as follows:

$$N'_i = (W_i - S_i.\sin\alpha_i - U_i.\cos\alpha_i).\sec\alpha_i \tag{8}$$

Factor of safety, FS_i, in terms of the local stress is defined as follows:

$$Fs_i = \frac{\tau_{fi}}{\tau_i} = \frac{S_{fi}}{S_i} \tag{9}$$

According to the Mohr-Coulomb failure envelope, the ultimate shear strength, S_{fi}, at the bottom of the slice i is expressed as follows:

$$S_{f_i} = \tau_{fi}.l_i = C_i + N'_i.\tan\phi \tag{10}$$

The shear stress-shear displacement, (τ_i)- Δ_i, relationship for the slice i derived from the hyperbolic equation is as follows:

$$\tau_i = \frac{\varepsilon_i}{a' + b'.\varepsilon_i} \tag{11}$$

$$\gamma_i = \frac{\Delta L_i}{L_{0i}} = \frac{\Delta_i}{L_{0i}} \tag{12}$$

$$\tau_i = \frac{\Delta}{a'L_{0_i} + b'.\Delta} \tag{13}$$

$$a' = \frac{1}{k_{initial}} \tag{14}$$

$$b' = \frac{R_f}{\tau_{fi}} \tag{15}$$

where
$k_{initial}$= The initial value of shear spring constant
R_f = failure ratio
With the normalization of Eq. (8) and the use of τ_{fi}, we have:

$$\frac{\tau_i}{\tau_{fi}} = \frac{\Delta_i}{aL_0 + b.\Delta_i} \tag{16}$$

Where

$$a = a'.\tau_{fi} = \frac{\tau_{fi}}{k_{initial}} \tag{17}$$

$$b = b'.\tau_{fi} = R_f \tag{18}$$

The initial modulus, $k_{initial}$, is assumed as an exponential function of the effective normal pressure, σ'_n, on the failure surface. According to the equations proposed by Duncan and Chang (1970), it can be written as:

$$k_{initial} = K.Pa.\left(\frac{\sigma'_{ni}}{Pa}\right)^n \tag{19}$$

$$\sigma'_{ni} = \frac{N'_i}{B_i.\sec\alpha_i} \tag{20}$$

where, k and n are material constants, P_a is atmospheric pressure, and B_i is thickness of the slice i.

The effect of normal stress on the relationship between τ_i and Δ_i is considered using Eqs. (8), (16), (17) and (18). Given the definition of the factor of safety in the Eqs. (9) – (16), then:

$$F_{S_i} = \frac{aL_0 + b.\Delta_i}{\Delta_i} \tag{21}$$

According to the displacement compatibility [21] shown in Figs. 2(a)-(b), then:

$$\Delta_2 = \Delta_1.\frac{\cos(\alpha_1 - 2\psi)}{\cos(2\psi - \alpha_2)} \tag{22}$$

where

ψ =dilation angle

The shear displacement of slice i in term of the vertical displacement at slope crest is written as follows:

$$\Delta_i = \Delta_1.\frac{\cos(\alpha_1 - 2\psi)}{\cos(2\psi - \alpha_i)} = \frac{\Delta_0}{\sin(\alpha_1 - \psi)}.\frac{\cos(\alpha_1 - 2\psi)}{\cos(2\psi - \alpha_i)} \tag{23}$$

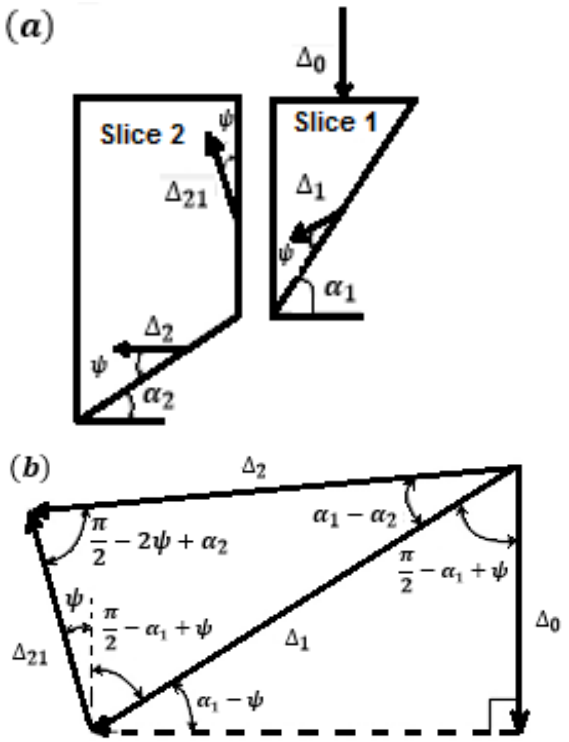

(a) Vectors of shear displacement
(b) Displacement diagram

Fig. 2: Displacement compatibility of adjacent slices [21]

The Eq. (23) can be rewritten as follows:

$$\Delta_i = \Delta_0.f(\alpha_i) \tag{24}$$

Where

$$f(\alpha_i) = \frac{1}{\sin(\alpha_1 - \psi)}.\frac{\cos(\alpha_1 - 2\psi)}{\cos(2\psi - \alpha_i)} \tag{25}$$

By substituting the Eq. (24) into the Eq. (21), one can write:

$$F_{S_i} = \frac{aL_0 + b.\Delta_0.f(\alpha_i)}{\Delta_0.f(\alpha_i)} \tag{26}$$

Considering equilibrium of forces in the horizontal direction, ($\sum F_H = 0$), one can write:

$$\sum\left(\frac{S_{fi}.\sec\alpha_i}{F_{S_i}}\right) = \left[\sum W_i.\tan\alpha_i\right] - E_{ns} + E_0 \tag{27}$$

Where

$$S_{fi} = \left(S_{fi}\right)_{residual} = \frac{C_i + \left(W_i - U_i.\cos\alpha_i\right).\tan\phi.\sec\alpha_i}{1 + \dfrac{\tan\phi.\tan\alpha_i}{F_{S_i}}} \quad (28)$$

$$\left(S_{fi}\right)_{mobilized} = \frac{S_{fi}}{F_{S_i}} = \frac{\left(S_{fi}\right)_{residual}}{F_{S_i}} \quad (29)$$

By substituting the Eqs. (26)- (28) into the Eq. (27), one can write:

$$\Delta_0.\sum\left[\frac{C_i + \left(W_i - U_i.\cos\alpha_i\right)\tan\phi.\sec\alpha_i}{1 + \dfrac{\tan\phi.\tan\alpha_i.\Delta_0.f\left(\alpha_i\right)}{aL_0 + b.\Delta_0.f\left(\alpha_i\right)}}\right].$$
$$\left[\frac{f\left(\alpha_i\right)}{aL_0 + b.\Delta_0.f\left(\alpha_i\right)}\right] = \left[\sum W_i.\tan\alpha_i\right] - E_{ns} + E_0 \quad (30)$$

The Eq. (30) in terms of Δ_0 can be written as follows:

$$\Delta_0 = \frac{\left[\sum W_i.\tan\alpha_i\right] - E_{ns} + E_0}{\sum\left[\dfrac{C_i + \left(W_i - U_i.\cos\alpha_i\right)\tan\phi.\sec\alpha_i}{1 + \dfrac{\tan\phi.\tan\alpha_i.\Delta_0.f\left(\alpha_i\right)}{aL_0 + b.\Delta_0.f\left(\alpha_i\right)}}\right].\left[\frac{f\left(\alpha_i\right)}{aL_0 + b.\Delta_0.f\left(\alpha_i\right)}\right]} \quad (31)$$

Next, the convergence Δ_0 can be controlled using the following criterion:

$$\varepsilon = \frac{\left(\Delta_0\right)_{new} - \left(\Delta_0\right)_{old}}{\left(\Delta_0\right)_{new}} \le 0.01 \quad (32)$$

If $\varepsilon \le 0.01$, then Δ_0 is considered as the vertical displacement at the slope crest, otherwise the procedure is repeated until the convergence is achieved.

2.4 Local factor of safety in term of displacement (FD_i)

The displacement of the failure surface (Δ_f) can be calculated by replacement of τ_i and Δ_i with τ_{fi} and Δ_f, respectively, in the Eq. (16) and considering $FS_i = 1$ in the Eq. (9):

$$F_{S_i} = 1 = \frac{aL_0 + b.\Delta_f}{\Delta_f} \quad (33)$$

$$\Delta_f = \frac{aL_0}{1 - b} \quad (34)$$

The local factor of safety, F_{Di}, in terms of displacement is defined as follows:

$$F_{D_i} = \frac{\Delta_f}{\Delta_i} \quad (35)$$

By substituting the Eqs. 24 to 34 into the Eq. (35), one can write:

$$F_{D_i} = \frac{aL_0}{\Delta_0.f\left(\alpha_i\right).(1 - b)} \quad (36)$$

An algorithm is coded in FORTRAN on the flow chart shown in Fig. 3.

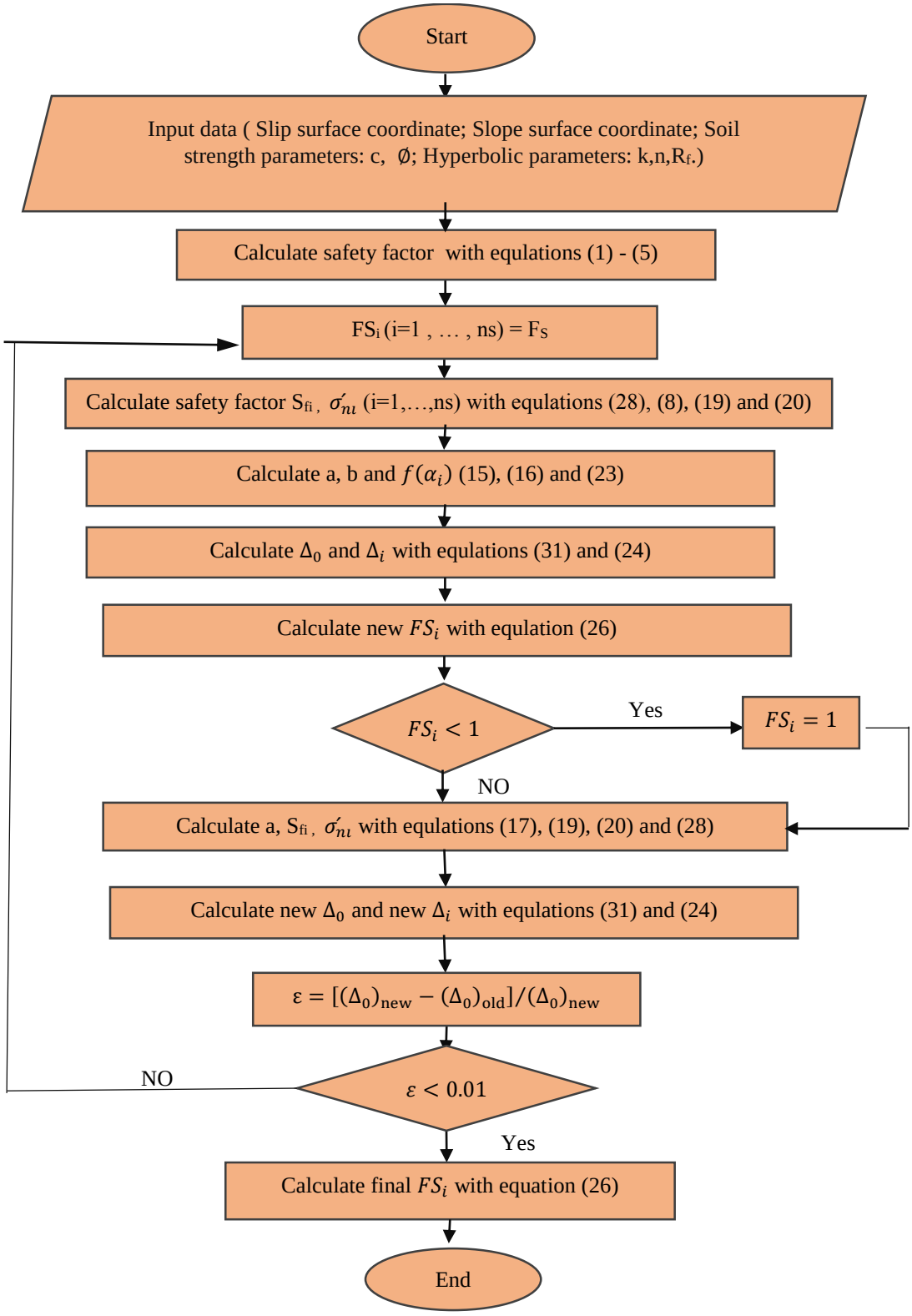

Fig. 3: Flowchart of the vertical displacement at the crown and shear displacement of slices

3. Examples

In order to examine the proposed method, two practical examples are presented in this paper. It is worth mentioning here that the considered examples are solved by a computer code created by the FORTRAN software.

3.1 Example 1

As shown in Fig. 4, in this example, an earth slope with a height of 100 m and a gradient of 2:1 was studied. Properties of the modeled slope are presented in Table 1.

Table 1. The specifications of the modeled slope

E	c	φ	ν	γ_d
30MPa	40kPa	26	0.3	20 kN/m^3

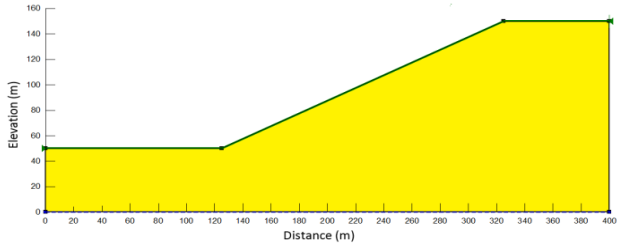

Fig. 4: Slope geometry

Fig. 5 displays a comparison between the shear displacements of different slices obtained from the present study and those obtained from the FEM analysis.

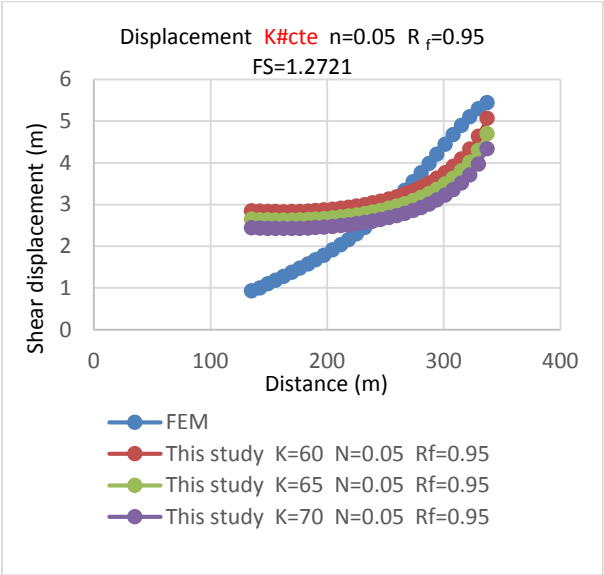

Fig. 5: Comparison of shear displacement of slices using FEM and proposed method on the slip surface

3.1.1 Calculation of the normal error

The normal error is calculated using the following equation:

$$e = \frac{1}{N}\sqrt{\frac{\sum_{i=1}^{n}\left((XY_{Shear})_i^{Num} - (XY_{Shear})_i^{Exact}\right)^2}{\sum_{i=1}^{n}\left((XY_{Shear})_i^{Exact}\right)^2}} \qquad (37)$$

Where, ň is the number of slices, $(XY_{Shear})^{Num}_{i}$ is the shear displacement obtained from the present study, $(XY_{Shear})^{Exact}_{i}$ is the shear displacement obtained from FEM, and e is the normal error.

Fig. 6 shows the shear displacements of slices for the hyperbolic stiffness parameters of K = 60, n = 0.05 and R_f = 0.95. As can be seen, the displacements obtained from this study were in good agreement with the displacements obtained from the FEM analysis. The normal error was equal to 1.066% which is acceptable.

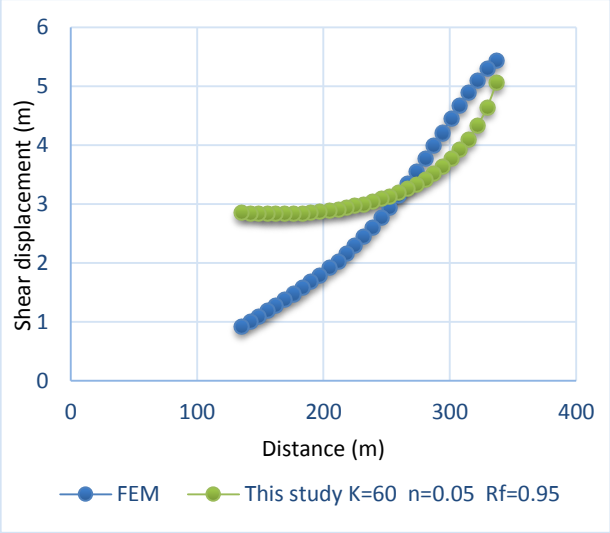

Fig. 6: Comparison of shear displacement of slices using the FEM and proposed method on the slip surface

Fig. 7 shows local factors of safety in terms of stress, (Fs_i), and displacement, (F_{Di}). The factors of safety in terms of displacement were significantly varying along the failure surface because of the nonlinear stress-displacement relationship. Therefore, the factor of safety in terms of the displacement showed the slope instability in a more realistic way. In Figs. 8-9, which respectively illustrate the outputs of the FEM analysis and the code written in FORTRAN, all parameters were constant and R_f (failure ratio) was changed. According to the Figs. 8-9, it can be concluded that with increasing failure ratio in the FEM, the displacement got increased very slightly, while with increasing failure ratio in the present study, the displacement got increased significantly.

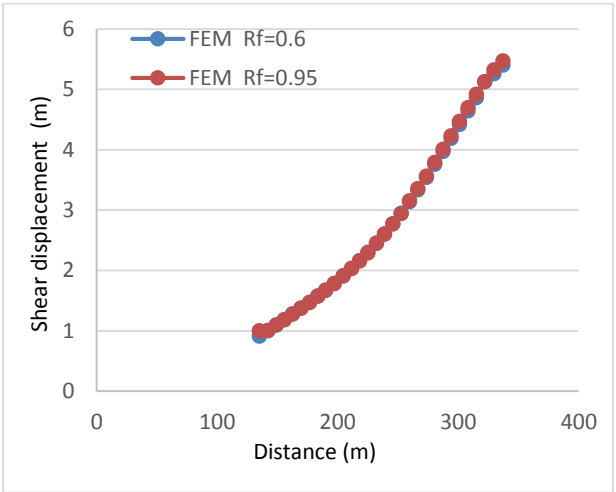

Fig. 8: Shear displacement of slices using FEM for Rf=0.6 and Rf=0.95 on the slip surface

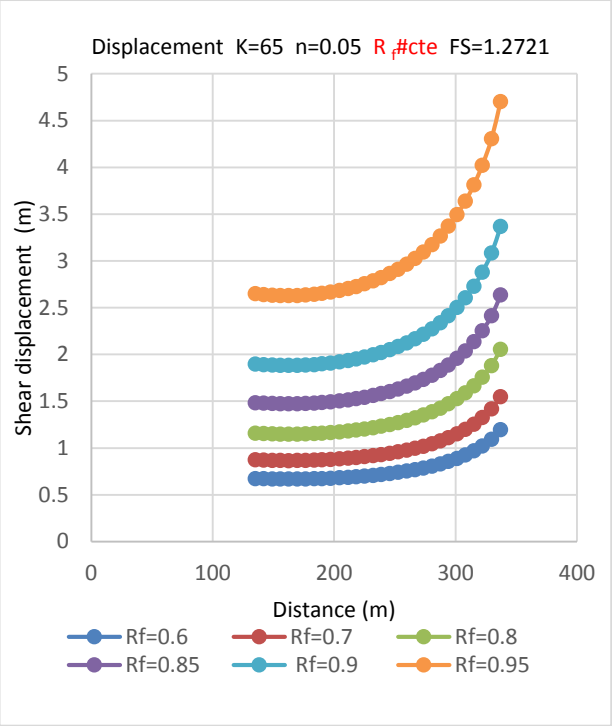

Fig. 9: Shear displacement of slices using proposed method for R_f=0.6, 0.7, 0.8, 0.85, 0.9, 0.95 on the slip surface

In Fig. 10 which shows the results obtained from the present study, all parameters were constant and only n was increased. It can be seen that with the increasing n, the displacement has been decreased.

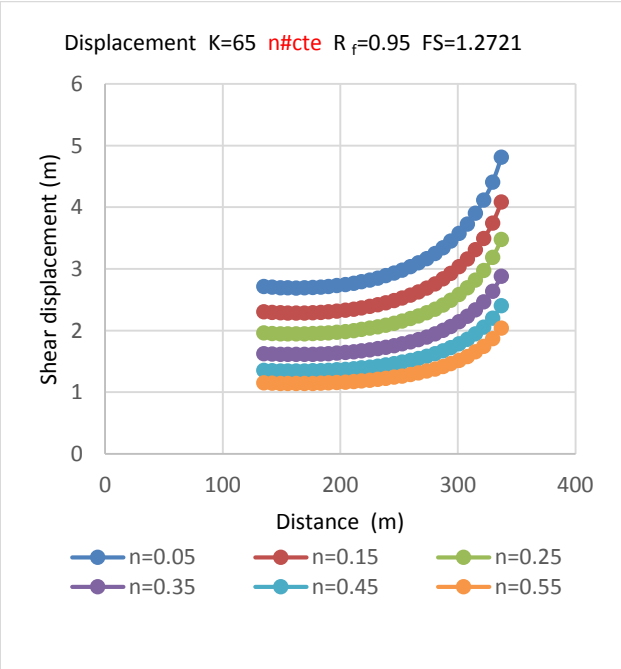

Fig. 10: Shear displacement of slices using proposed method for n=0.05, 0.15, 0.25, 0.35, 0.45, 0.55 on the slip surface

In Fig. 11, which shows the results obtained from the present study, all parameters were constant and only k (stiffness number) was changed. This diagram indicates that by increasing k, the displacement has got decreased.

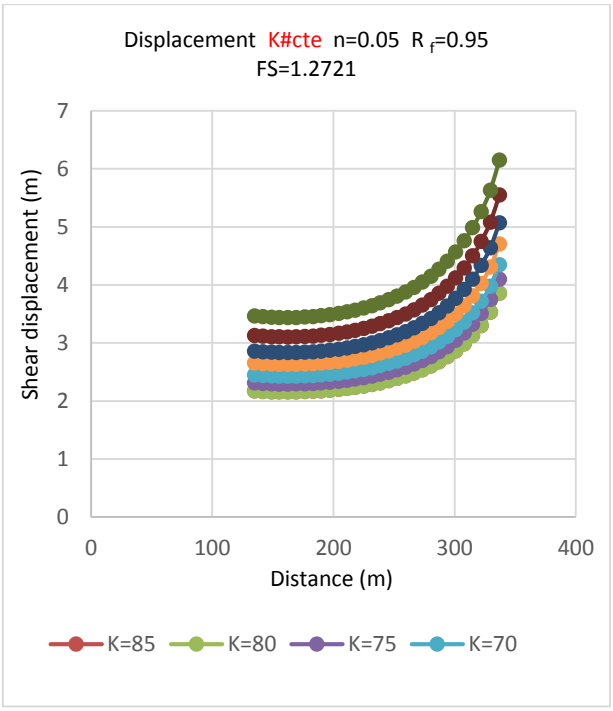

Fig. 11: Shear displacement of slices using proposed method for K=50, 55, 60, 65, 70, 75, 80, 85 on the slip surface

3.2 Example 2

As shown in Fig. 12, in this example, an earth slope with a height of 20 m and a slope angle of 45 degrees was studied. Properties of the slope are presented in Table 2.

Table 2. The specifications of the modeled slope

E	c	φ	ν	γ_d
1118MPa	55kPa	26	0.3	20 kN/m^3

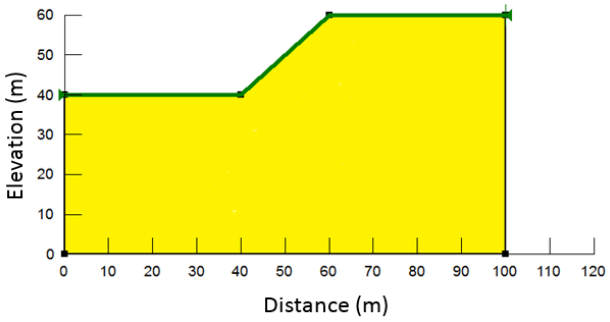

Fig. 12: Slope geometry

Fig. 13 shows a comparison between the shear displacements obtained from the present study and those obtained from the FEM analysis. It is verified that the obtained shear displacements in the crown and the toe of

the slope are in compliance with those obtained using the FEM analysis. However, it should be noted that the compliance in the other slices are less. The obtained shape using the proposed method is similar to the slip surface of slope whereas the obtained shape using the FEM analysis is to be about linear. It seems that the shape of the proposed method has a better description of the shear displacement on the slip surface than the FEM.

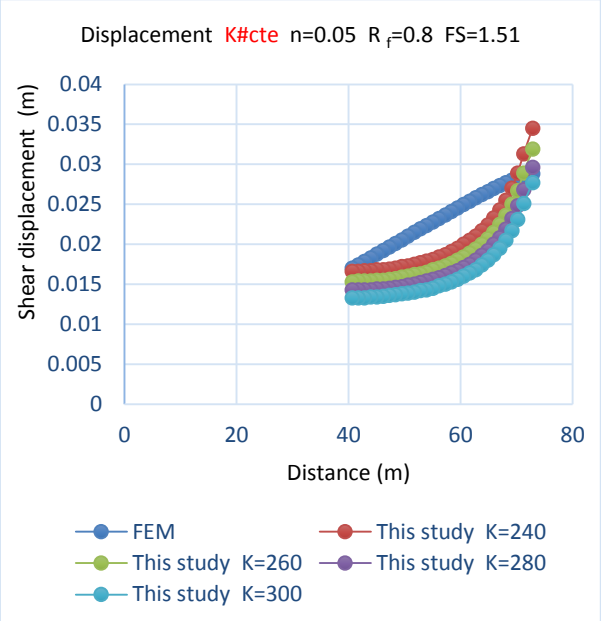

Fig. 13: Comparison of shear displacement of slices using FEM and proposed method on the slip surface

Fig. 14 illustrates shear displacements of slices for the hyperbolic stiffness parameters of K =240, n = 0.05 and Rf= 0.8. Examining Fig. 14, it is verified that the obtained shear displacements in the crown and the toe of slope are in compliance with those obtained using the FEM analysis. However, it should be noted that the good agreement in other slices are less. The obtained shape using proposed method is similar to slip surface of slope whereas the obtained shape using the FEM analysis is about linear. It seems that the shape of the proposed method has a better description of the shear displacement on the slip surface than the FEM analysis. The normal error was equal to 0.52% which is acceptable.

Fig. 15 shows local factors of safety in terms of stress, (Fs_i), and displacement, (F_{Di}). The factors of safety in terms of displacement were significantly varied along the failure surface.

In Fig. 16, all parameters were constant and only $R_f$was varied. It can be seen that with increasing failure ratio, displacement was increased.

In Fig. 17, all parameters were constant and only n was increased. It can be seen that with increasing n, displacement was decreased.

In Fig. 18, all parameters were constant and only k (stiffness number) was varied. This diagram indicates that with increasing k, displacement was decreased.

.

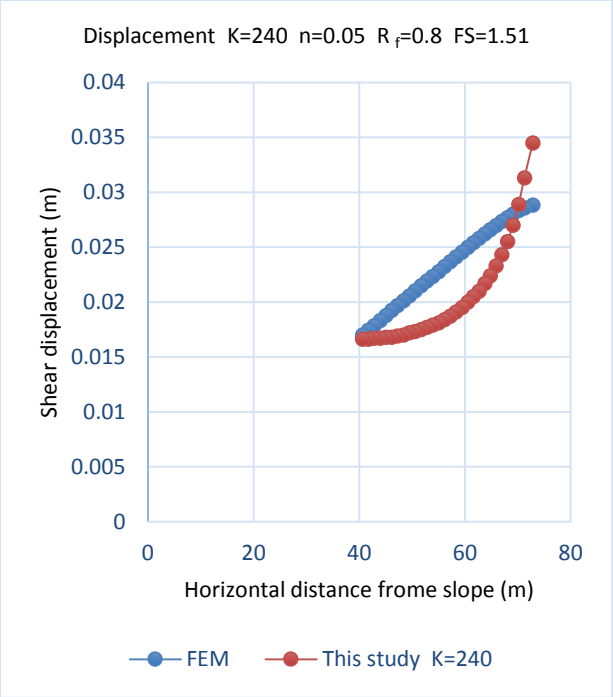

Fig. 14: Comparison of shear displacement of slices using the FEM analysis and proposed method on the slip surface

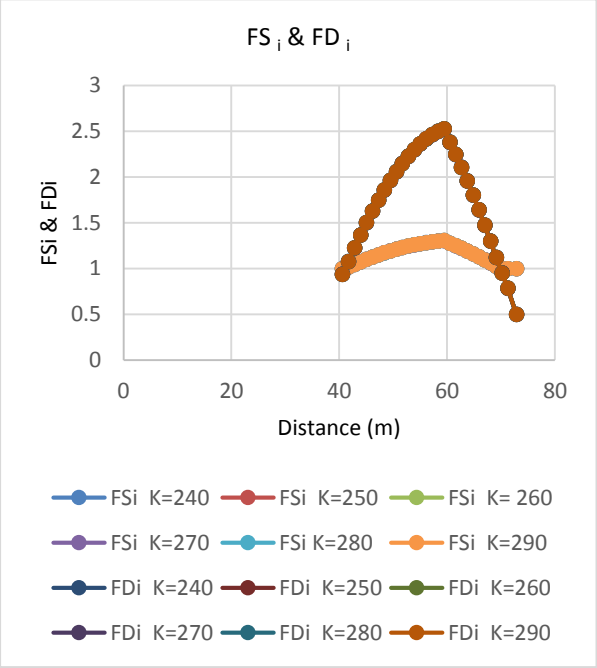

Fig. 15: Local factor of safety in term of stress (FS_i) and displacement (FD_i) on the slip surface

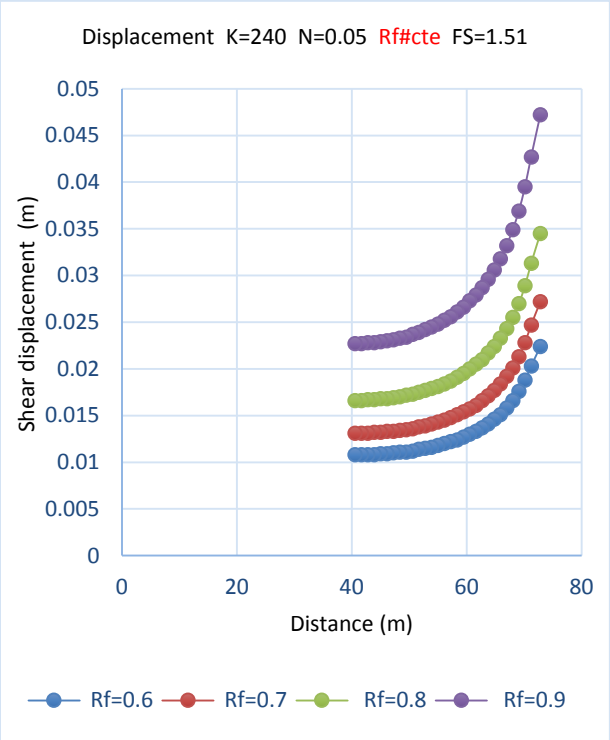

Fig. 16: Local factor o Figure16. Shear displacement of slices using proposed method for R_f=0.6, 0.7, 0.8, 0.9 on the slip surface

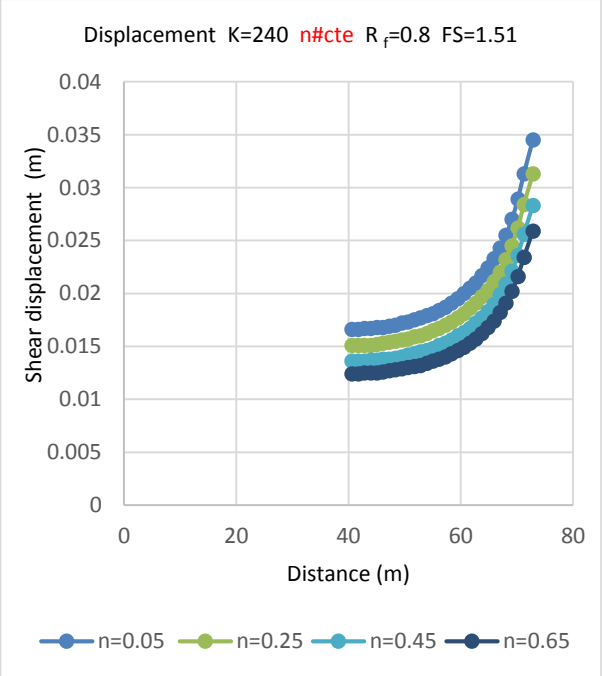

Fig. 17: Shear displacement of slices using proposed method for n=0.05, 0.25, 0.45, 0.65 on the slip surface

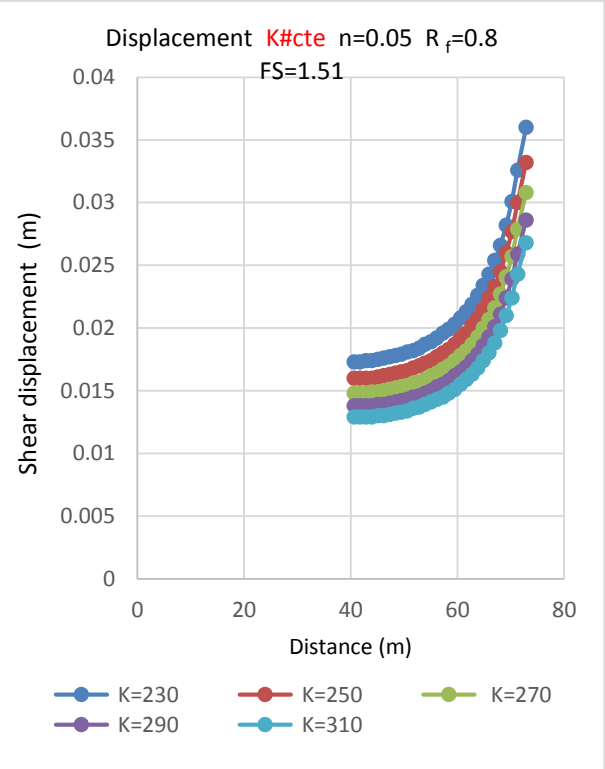

Fig. 18: Shear displacement of slices using proposed method for K=230, 250, 270, 290, 310 on the slip surface

4. Conclusions

In the present study, a novel method was proposed to calculate the displacement of failure surface in earth slopes. The failure surface can be circular or non-circular. In this regard, a numerical model was developed and the following results were obtained:

The displacements obtained from this study were in good agreement with the displacements obtained from the FEM analysis. The normal errors in Examples 1 and 2, were equal to 1.066% and 0.52%, respectively which are acceptable.

The local factors of safety in terms of stress, (Fs_i), and displacement, (F_{Di}) were calculated for the failure surface. It was observed that the factors of safety in terms of the displacement were significantly varying along with the failure surface because of the nonlinear stress-displacement relationship. Therefore, the factors of safety in terms of the displacement showed a slope instability in a more realistic way.

The effects of R_f, n, and k were examined and the following results were obtained:

- With increasing R_f in the FEM analysis, displacement was increased very slightly, while with increasing R_f in the present study, displacement was increased significantly. decreased.
- With increasing n, displacement was decreased.

- With increasing k, displacement was decreased.

References

[1] Duncan, J.M. and Wright, S.G. (2005), Soil Strength and Slope Stability. Chapter 6: Mechanics of Limit Equilibrium Procedures, John Wiley & Sons Ltd., 55-102.

[2] Kahatadeniya, K.S., Nanakorn, P., Neaupane, K.M. (2009), "Determination of the critical failure surface for slope stability analysis using ant colony optimization", Eng. Geo., 108, 133–141. doi.org/10.1016/j.enggeo.2009.06.010.

[3] Mendoza, F.J.C., Gisbert, A.F., Izquierdo, A.G., Bovea, M.D. (2009), "Safety factor nomograms for homogeneous earth dams less than ten meters high", Eng. Geo., 105, 231–238. doi: 10.1016/j.enggeo.2009.01.001.

[4] Di Maio, C., Vassallo, R., Vallario, M., Pascale, S., Sdao, F. (2010), "Structure and kinematics of a landslide in a complex clayey formation of the Italian southern Apennines", Eng. Geo., 116, 311–322. DOI: 10.1016/j.enggeo.2010.09.012.

[5] Ferrari, A., Ledesma, A., Gonzalez, D.A., Corominas, J. (2011), "Effects of the foot evolution on the behaviour of slow-moving landslides", Eng. Geo., 117, 217–228. doi: 10.1016/j.enggeo.2010.11.001.

[6] Zheng, H., (2012), "A three-dimensional rigorous method for stability analysis of landslides", Eng. Geo., 145–146, 30–40. doi.org/10.1016/j.enggeo.2012.06.010.

[7] Huang, Ch-Ch. (2013), "Developing a new slice method for slope displacement analyses", Eng. Geo, 157(1), 39-47. doi: 10.1016/j.enggeo.2013.01.018.

[8] Huang, Ch-Ch. (2014), "Force equilibrium-based finite displacement analyses for reinforced", Geotext. Geomembr, 42, 394-440. https://doi.org/10.1016/j.geotexmem.2014.06.004.

[9] Huang, Ch-Ch., and Hsieh H-Y., and Hsieh Y-L. (2014), "Slope displacement analyses using force equlibrium-based finite displacement method and circular failure surface", Journal of GeoEng., 9(1), 11-19. dx.doi.org/10.6310/jog.2014.9(1).2

[10] Mohammadi, S., and Taiebat,H. (2013), "A large deformation analysis for the assessment of failure induced deformations of slopes in strain softening materials", Comput. & Geotech., 49, 279–288. doi.org/10.1016/j.compgeo.2012.08.006.

[11] Cheng, H, and Zhou, X. (2015), "A novel displacement-based rigorous limit equilibrium method for three-dimensional landslide stability analysis" Can.Geotech., 52(12), 2055-2066. doi.org/10.1139/cgj-2015-0050.

[12] Ghanbari, A., Khalilpasha, A., Sabermahani, M. and Heydari, B. (2013) "An analytical technique for estimation of seismic displacements in reinforced slopes based on horizontal slices method (HSM)" Geomechanics and Engineering, An Int'l Journal, 5(2), doi: 10.12989/gae.2013.5.2.143

[13] Gao, w., and He T.Y. (2017) "Displacement prediction in geotechnical engineering based on evolutionary neural network" Geomechanics and Engineering, An Int'l Journal 13(5),):845-860. doi:10.12989/gae.2017.13.5.845.

[14] Zhang, G., Tan, J., Zhang, L., and Xiang, Y. (2015) "Linear regression analysis for factors influencing displacement of high-filled embankment slopes", Geomechanics and Engineering, An Int'l Journal 8(4), 511-521 .doi.org/10.12989/gae.2015.8.4.511

[15] Aminpour, M.M, Maleki, M., Ghanbari, A. (2017), "Investigation of the effect of surcharge on behavior of soil slopes" Geomechanics and Engineering, An Int'l Journal, 13(4), 653-669. DOI: 10.12989/gae.2017.13.4.653.

[16] Hasani, N., Ghanbari, A., Hosseini, S. (2014) " Analytical estimation of natural frequency in earth dams with respecting to the foundation effects", Numerical Methods in Civil Engineering, Vol. 1, No.1,September.2014

[17] Macedo, J., Bray, J., Abrahamson, N., Travasarou, T. (2018), "Performance-Based Probabilistic Seismic Slope Displacement Procedure", Earthquake Spectra, May 2018, Vol. 34, No. 2, pp. 673-695. doi.org/10.1193/122516EQS251M

[18] Kokusho, T.(2019) "Energy-Based Newmark Method for earthquake-induced slope displacements", Soil Dynamics and Earthquake Engineering, Volume 121, June 2019, Pages 121-134. doi.org/10.1016/j.soildyn.2019.02.027

[19] Liu, ch., Jiang, Zh., Han, X., Zhou, W (2019), "Slope displacement prediction using sequential intelligent computing algorithms", Measurement, Volume 134, February 2019, Pages 634-648. doi.org/10.1016/j.measurement.2018.10.094

[20] Janbu, N. (1973), "Slope stability computations, Embankment-Dam Engineering", In: Hirschfeld, R.C., Poulos, S.J. (Eds.), Casagrande Volume. John Wiley & Sons, pp. 47–86.

[21] Atkinson, J.H. (1981), Foundations and Slopes: An Introduction to Applications of Critical State Soil Mechanics, McGraw-Hill, London.